http://ansinet.com/itj

ITJ

ISSN 1812-5638

INFORMATION TECHNOLOGY JOURNAL

ANSInet
Asian Network for Scientific Information
308 Lasani Town, Sargodha Road, Faisalabad - Pakistan

Information Technology Journal 12 (21): 6481-6486, 2013
ISSN 1812-5638 / DOI: 10.3923/itj.2013.6481.6486

High Order Regularization for Mr Image Denoising

[1]Shisong Zhu, [1]Bibo Lu and [2]Cuiyun Zhang
[1]School of Computer Science and Technology, Henan Polytechnic University, Henan, Jiaozuo, 454003, China
[2]Henan College of Industry and Information Technology, Henan, Jiaozuo, 454000, China

Abstract: Magnetic Resonance (MR) image have been widely used and plays an important role in a clinical diagnosis. We focus on the denoising of MR image with a new high order regularization model. Contrary to previous fourth order models, the proposed energy functional contains the first order derivatives as boundary detector. The corresponding Euler-Lagrange equation can adjust diffusion speed adaptive to the local structure. The experimental results on the MR image show the performance of the proposed method. The effect of varying the high order regularization parameter is also reported.

Key words: Magnetic resonance image, high order model, edge preserving, regularization

INTRODUCTION

Magnetic resonance image have been widely used and plays an important role in a clinical diagnosis. High quality MR image is helpful to make an accurate and fast estimation for patient situation. However, there is a tradeoff between Signal-noise-ratio (SNR), spatial resolution and acquisition time. The current MRI can be divided two regimes: high SNR and high resolution with low SNR imaging. To obtain a higher resolution image with a high SNR, more acquisition time is needed. As MR images are affected by several artifacts and noise sources and one of them is the random fluctuation of MRI signal, one can obtain a high quality MR image by averaging over repeated measurements (Lysaker *et al*., 2003). Though this method can promise us with ”idea” or ”true” image, it may be limited by parameters such as the patient comfort or by physiological constraints (Krissian and Aja-Fernndez, 2009). Efficient post-processing methods are still needed to reduce the noise in original MR images. Several filtering technologies have been proposed to reduce noise in MRI. Henkelman tried to estimate the magnitude MR image from a noisy image. Sijbers *et al*. estimated the Rician noise level and perform signal reconstruction using a maximum likelihood approach (Sijbers and den Dekker, 2004). Application of wavelets for denoising of MR images has been pioneered by (Weaver *et al*., 1991). They applied their scheme on MR images of the human neck which reduced noise from 10 to 50 without reducing edge sharpness. An article by Wood and Johnson (1999) employed wavelet packets to remove the noise of MR date but this method would induce the distortions of both phase and amplitude. Filter technologies in wavelet domain have also been invested (Pizurica *et al*., 2003; Awate and Whitaker, 2007). A recent work reported the application of wavelet for 3D MRI denoising (Ogier *et al*., 2006).

Nonlinear diffusion filters have also been applied to remove noise in MR images. The major advantage of this method is its edge-preserving ability. The images are filtered by examining their evolutions under nonlinear PDEs. In contrast to linear diffusion filtering, i.e., Gaussian filtering, which is hampered with blurring and localization problems, the nonuniform (anisotropic) process reduces the diffusivity at locations which have a larger likelihood of being edges by using the edge-stopping function. This idea was introduced by Perona and Malik (1990). Their diffusion may be forward in homogeneous region or backward near edges, by setting a threshold K as a criterion. Another important PDE model is TV model (Rudin *et al*., 1992), which has proven to be a valuable method to the recovery of images. These second order PDE model has been generalized to 3-D images by Gerig *et al*. (1992) and to vector-valued images by Sapiro and Ringach in (Sapiro and Ringach, 1996), making it suitable to both 3-D MRI and multi-spectral MRI.

Although these second order nonlinear models have been demonstrated to be able to achieve a good trade-off between noise removal and edge preservation, they tend to cause the processed image to look ”blocky”, that is staircase (Chambolle and Lions, 1997). To overcome the staircase produced by the second order models, You and Kaveh (2000) presented a fourth-order PDE which is derived by minimizing an energy functional of the image Laplacian. Lysaker *et al*. (2003) proposed another fourth order approach (LLT) and applied it to the denoising of

Corresponding Author: Bibo Lu, School of Computer Science and Technology, Henan Polytechnic University, Henan, Jiaozuo, 454003, China

the MR image in space and time. Though these new fourth order model reduce the staircase in the denoised image, they have the disadvantage of blurring edges. The essential reason for the blurring of the edges is that these PDEs evolve mainly depending on the second order derivation of the image, which can not locate the position of edges in a noise image. To overcome this problem, some new models were also proposed in (Lu and Liu, 2010; Kim and Lim, 2009; Lysaker and Tai, 2006; Zhu and Chan, 2012).

In this study, we propose a new fourth order model and conduct a further investigation in the regularization technique. The difference scheme is also given and the experimental results on MR data are demonstrated.

FOURTH ORDER REGULARIZATION MODEL FOR MRI DENOISING

The mathematics formulation of MR image noise: As the magnitude of the MRI signal is the square root of the sum of the squares of Gaussian distributed real and imaginary parts, the noise in data is considered as a Rician distribution (Sijbers and den Dekker, 2004). The Rician distribution tends to a Rayleigh distribution in a low intensity regions of the image. In high intensity regions, where most important information lies, it approaches to a Gaussian distribution. Therefor, we approximately consider the noise in MR image as an additive noise model as:

$$u_0(x, y) = u(x, y)+\eta(x, y) \tag{1}$$

where, $u(x, y)$ is a digital MR image and $u_0(x, y)$ be its observation data with random noise $\eta(x, y)$ for $(x, y)\epsilon\Omega$. Our aim is to restore MR image u from the observed noisy data u_0. Assume the noise level is approximately known, i.e.:

$$\int_\Omega (u-u_0)^2\, dxdy = \sigma^2 \tag{2}$$

Fourth order regularization method: Researchers utilized a great deal PDEs to remove noise in MRI data. Most of the equations are associated with certain energy functional. Lysaker *et al.* (2003) considered a high order (LLT) model for MR image denoising as follows:

$$E(u) = \int_\Omega (|u_{xx}| + |u_{yy}|)dxdy \tag{3}$$

This model can remove noise and recovery a smoothing region in MR image. However, it is found that it tends to blur edges. As an important feature, the edges implies important clues for diagnosis, it is critical to protect edges in MR image. Considering the edge preserving ability of total variation model, some combination of TV model and fourth order models were presented in (Chan *et al.*, 2000) and (Lysaker and Tai, 2006). In these methods, weight functions were needed to balance the trade-off between two models. We propose a new energy functional as follows:

$$E(u) = \int_\Omega \frac{|u_{xx}| + |u_{xy}| + |u_{yx}| + |u_{yy}|}{|\nabla u_\sigma|} dxdy \tag{4}$$

Where:

$$|\nabla u| = \sqrt{u_x^2 + u_y^2}$$

and u_σ denotes the convoluting of u with a Gaussian kernel σ. By introducing the gradient information with, it is helpful to detect object boundaries. The convolution of u is to reduce the variation of gradient brought by noise. A technique for finding minimum value of E(u) subject to the noise level constrain Eq. 2 is based on a Lagrangian functional:

$$E(u) = \int_\Omega \frac{|u_{xx}| + |u_{xy}| + |u_{yx}| + |u_{yy}|}{|\nabla u_\sigma|} dxdy + \frac{\lambda}{2}\int_\Omega (u-u_0)^2 dxdy \tag{5}$$

where, $\lambda \geq 0$ is Lagrange multiplication. The first term on the right-hand side of Eq. 5 is to measure the oscillations in the image, the second term is to measure the identification between u and u0. At any critical point of E(u) we must have:

$$\frac{\partial E}{\partial u} = 0 \tag{6}$$

From Eq. 5 and 6, we can calculate the following Euler-Lagrange equation:

$$\left(\frac{u_{xx}}{|\nabla u_\sigma||u_{xx}|}\right)_{xx} + \left(\frac{u_{xy}}{|\nabla u_\sigma||u_{xy}|}\right)_{xy} + \left(\frac{u_{yx}}{|\nabla u_\sigma||u_{yx}|}\right)_{yx} + \left(\frac{u_{yy}}{|\nabla u_\sigma||u_{yy}|}\right)_{yy} + \lambda(u-u_0) = 0 \tag{7}$$

To solve the nonlinear Eq. 7, we introduce an artificial time and obtain a fourth order adaptive method:

$$u_t = -\left(\frac{u_{xx}}{|\nabla u_\sigma||u_{xx}|}\right)_{xx} - \left(\frac{u_{xy}}{|\nabla u_\sigma||u_{xy}|}\right)_{xy} - \left(\frac{u_{yx}}{|\nabla u_\sigma||u_{yx}|}\right)_{yx} - \left(\frac{u_{yy}}{|\nabla u_\sigma||u_{yy}|}\right)_{yy} - \lambda(u - u_0) \quad (8)$$

The LLT model leads to the fourth order evolution equation as:

$$u_t = -\left[\left(\frac{u_{xx}}{|u_{xx}|}\right)_{xx} + \left(\frac{u_{yy}}{|u_{yy}|}\right)_{yy}\right] - \lambda(u - u_0) \quad (9)$$

The essential difference between our time-depend Eq. 8 and LLT Eq. 9 is the control of the diffusion. The diffusion speed of LLT depends on the sign of the second order derivative u_{xx} and u_{yy}. In our scheme, the diffusion speed not only depends on the sign of the second derivative u_{xx} and u_{yy} but also depends on the amount of the boundary detection function $|\Delta u_\sigma|$, which is larger near the edge. Our approach adjusts the diffusion speed adaptively according to the local structure of the image to protect more details.

The boundary condition of Eq. 8 is:

$$\frac{\partial u}{\partial u} = 0 \quad (10)$$

and the initial condition is:

$$u(x, 0) = u_0 \quad (11)$$

where, n is unit outward normal direction on $\partial\Omega$.

Difference schemes: The differential Eq. 8 may be solved numerically using an iterative approach. For the initial image u_0 with support $I \times J$, assuming a time step size of Δt and a space grid size of $h = 1$. For time discretion:

$$u_t \approx \frac{u^{l+1} - u^l}{\Delta t} \quad (12)$$

Using central difference to approximate first order derivatives:

$$D_x(u_{i,j}) = \frac{u_{i+1,j} - u_{i-1,j}}{2}, D_y(u_{i,j}) = \frac{u_{i,j+1} - u_{i,j-1}}{2}$$

and second order derivatives:

$$\begin{aligned} D_{xx}(u_{i,j}) &= u_{i+1,j} + u_{i-1,j} - 2u_{i,j}, \\ D_{yy}(u_{i,j}) &= u_{i,j+1} + u_{i,j-1} - 2u_{i,j}, \\ D_{xy}(u_{i,j}) &= D_{yx}(u_{i,j}) \\ &= \frac{u_{i+1,j+1} + u_{i-1,j-1} + u_{i-1,j+1} + u_{i+1,j-1}}{4} \end{aligned} \quad (13)$$

For boundary detection function g,

$$g_{i,j} = \varepsilon_{ig} + (D_{ix}(u_{\sigma,i,j}))^2 + (D_y(u_{\sigma,i,j}))^{1/2}$$

where ε is a small positive number in case to divided by zero and $u_{\sigma,i,j}$ denotes the pixel value in the point (i, j) of u_σ.

For Eq. 8:

$$\begin{aligned} u_{i,j}^{l+1} = u_{i,j}^l &- \Delta t D_{xx}(\alpha_\varepsilon^l D_{xx}(u_{i,j}^l)) \\ &- 2\Delta t D_{xy}(\beta_\varepsilon^l D_{xy}(u_{i,j}^l)) \\ &- \Delta t D_{yy}(\gamma_\varepsilon^l D_{yy}(u_{i,j}^l)) \\ &- \Delta t \lambda^l (u_{i,j}^l - u_{i,j}^0) \end{aligned} \quad (14)$$

In Eq. 14, α_ε, β_ε and γ_ε are calculated respectively as:

$$\alpha_\varepsilon(u_{i,j}) = \frac{1}{g_{i,j}(|D_{xx}(u_{i,j})| + \varepsilon)},$$

$$\beta_\varepsilon(u_{i,j}) = \frac{1}{g_{i,j}(|D_{xy}(u_{i,j})| + \varepsilon)},$$

$$\gamma_\varepsilon(u_{i,j}) = \frac{1}{g_{i,j}(|D_{yy}(u_{i,j})| + \varepsilon)}$$

where, ε is a regularization parameter to avoid numerical divisions by zero numbers.

EXPERIMENTAL RESULTS

In this section, we will show the denoising of MR image with our method. To make comparisons, we also provide the results of another fourth order LLT method. In our experimental, we will adopt different regularization parameters to investigate their influence to the denoising. There are two regularization parameters in the numerical scheme of the proposed methods. The first one is ε_g, for the low order regularization. The second one is ε, for the high order regularization. The research on ε_g have been reported in previous publications. Therefore, we focus on our attentions on the second order regularization, by fixing $\varepsilon_g = 0.1$.

Figure 1 shows the denoising results of T-2 noisy weight MR image (SNR = 10.9). The result by LLT method (SNR = 15.0) still remains some noise and edges are destroyed. Our method (SNR = 15.7, $\varepsilon = 1$) shows a good performance on both noise removal and edge preserving. In the difference images, the removed parts are shown after adjusted to mid-tone. Edges are more visible in LLT model.

We use the plastic straws MR phantom to test the denoisers preservation of edge information with two methods. The idea MR image can be obtained by

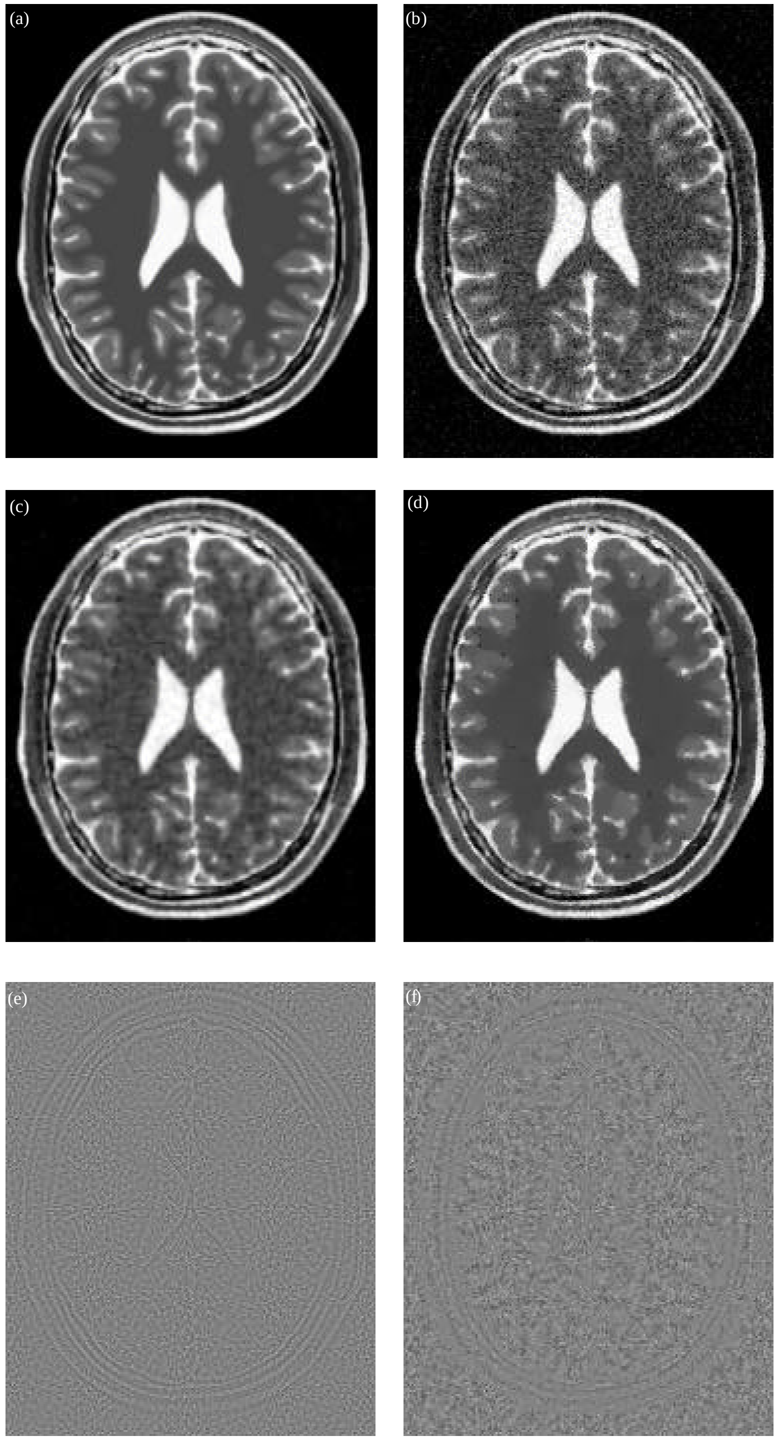

Fig. 1(a-f): T-2 weight image denoising, (a) Original image, (b) Noise image, (c) LLT result, (d) FOA result, (e) LLT difference image and (f) FOA difference image

averaging 4 repeated measurements. Figure 2a shows the noisy image, which is just the first one of the four images. The visual effect of our method is better than that of LLT, especially in smoothing area and edges. To further investigate the situation with different regularization parameters, the experimental results with different ε are

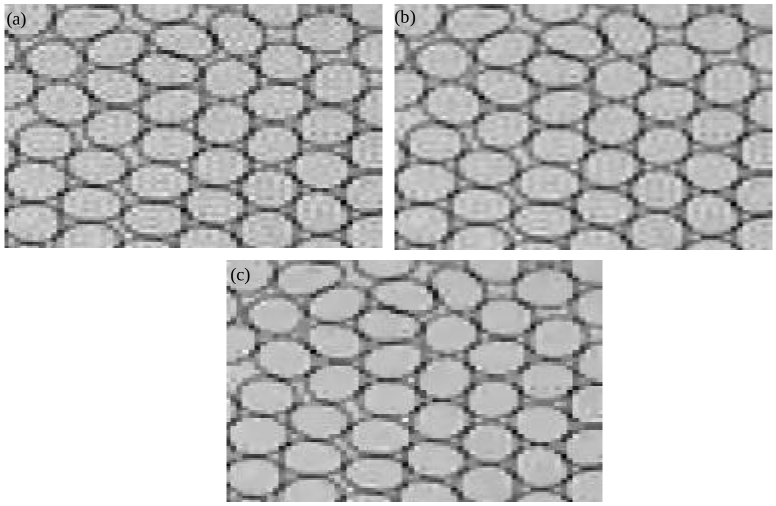

Fig. 2(a-c): Plastic straws MR phantom image denosing, (a) Noisy MR image, (b) LLT method and (c) Our method, $\varepsilon = 1$

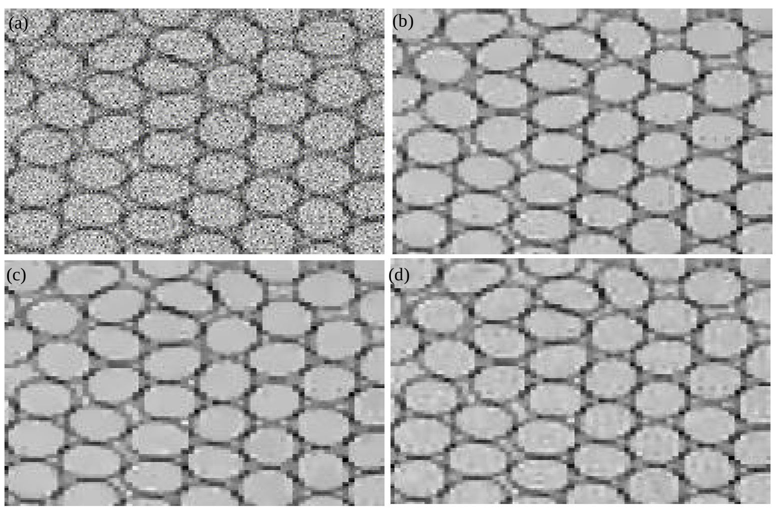

Fig. 3(a-d): Results with different high order regularization parameters, (a) $\varepsilon = 0.01$, (b) $\varepsilon = 0.1$, (c) $\varepsilon = 1$ and (d) $\varepsilon = 10$

shown in Fig. 3. The denoised images demonstratethe effect of different parameters. It seem that the parameters near 1 provides a more pleasant recovery image, which is coincide with the report in (Lu and Liu, 2010). In future work, we will further investigate the inter-effect of the first order regularization and the second regularization.

CONCLUSION

This study presents a new fourth order model for MR image denoising. The model is derived from a new energy functional. The induced fourth order diffusion model can preserve edges and smoothing transition region while denoising. Two regularization parameters are needed when considering numerical calculations. We investigates the choice of the second order regularization parameter. The experimental results on MR image show the performance of the proposed method.

ACKNOWLEDGMENTS

This study was supported by NSFC(10826042), The Doctor Grant of Henan Polytechnic University(B2009-41, B2010-95), The key young teacher programming, Projects of International Cooperation and Exchanges of Henan Province (084300510065), Foundation of Henan Educational Committee(13A520340), Natural Science Foundation of Jiangsu Province of China(BK20130235).

REFERENCES

Awate, S.P. and R.T. Whitaker, 2007. Feature-preserving MRI denoising: A nonparametric empirical bayes approach. IEEE Trans. Med. Imaging, 26: 1242-1255.

Chan, T., A. Marquina and P. Mulet, 2000. High-order total variation-based image restoration. SIAM J. Scientific Comput., 22: 503-516.

Chambolle, A. and P.L. Lions, 1997. Image recovery via total variation minimization and related problems. Numer. Math, 76: 167-188.

Gerig, G., O. Kubler, R. Kikinis and F. Jolesz, 1992. Nonlinear anisotropic filtering of MRI data. IEEE Trans. Med. Imaging, 11: 221-232.

Kim, S. and H. Lim, 2009. Fourth-order partial differential equations for effective image denoising. Electron. J. Different. Equat., 17: 107-121.

Krissian, K. and S. Aja-Fernandez, 2009. Noise-driven anisotropic diffusion filtering of MRI. IEEE Trans. Med. Imaging, 18: 2265-2274.

Lu, B.B. and Q. Liu, 2010. Image restoration with surface-based fourth-order partial differential equation. Proceedings of the SPIE International Society for Optical Engineering: Visual Communications and Image Processing, July 11-14, 2010, Huangshan, China.

Lysaker, M., A. Lundervold and X.C. Tai, 2003. Noise removal using fourthorder partial differential equation with applications to medical magnetic resonance images in space and time. IEEE Trans. Image Process., 12: 1579-1590.

Lysaker, M. and X.C. Tai, 2006. Iterative image restoration combining total variation minimization and a second-order functional. Int. J. Comput. Vision, 66: 5-18.

Ogier, A., P. Hellier and C. Barillot, 2006. Restoration of 3D medical images with total variation scheme on wavelet domains (TVW). Proceedings of the SPIE Medical Imaging: Image Processing, February 11-16, 2006, San Diego, USA., pp: 465-473.

Perona, P. and J. Malik, 1990. Scale-space and edge detection using anisotropic diffusion. IEEE Trans. Pattern Anal. Mach. Intell., 12: 629-639.

Pizurica, A., W. Philips, I. Lemahieu and M. Acheroy, 2003. A versatile wavelet domain noise filtration technique for medical imaging. IEEE Trans. Med. Imag., 22: 323-331.

Rudin, L.I., S. Osher and E. Fatemi, 1992. Nonlinear total variation based noise removal algorithms. Physica D Nonlinear Phenomena, 60: 259-268.

Sapiro, G. and D.L. Ringach, 1996. Anisotropic diffusion of multivalued images with applications to color filtering. IEEE Trans. Image Process., 5: 1582-1586.

Sijbers, J. and A.J. den Dekker, 2004. Maximum likelihood estimation of signal amplitude and noise variance from MR data. Magnet. Resonan. Med., 51: 586-594.

Weaver, J.B., Y. Xu, D.M. Healy Jr. and L.D. Cromwell, 1991. Filtering noise from images with wavelet transforms. Magn. Reson. Med., 21: 288-295.

Wood, J.C. and M.K. Johnson, 1999. Wavelet packet denoising of magnetic resonance images: Importance of Rician noise at low SNR. Magnet. Resonan. Med., 41: 631-635.

You, Y.L. and M. Kaveh, 2000. Fourth-order partial differential equations for noise removal. IEEE Trans. Image Process., 9: 1723-1730.

Zhu, W. and T. Chan, 2012. Image denoising using mean curvature of image surface. SIAM J. Imaging Sci., 5: 1-32.